

Multi-Agent Deep Reinforcement Learning For Optimising Energy Efficiency of Fixed-Wing UAV Cellular Access Points

Boris Galkin, Babatunji Omoniwa, and Ivana Dusparic

CONNECT- Trinity College Dublin, Ireland

E-mail: {galkinb, omoniwab, duspari}@tcd.ie

Abstract—Unmanned Aerial Vehicles (UAVs) promise to become an intrinsic part of next generation communications, as they can be deployed to provide wireless connectivity to ground users to supplement existing terrestrial networks. The majority of the existing research into the use of UAV access points for cellular coverage considers rotary-wing UAV designs (i.e. quadcopters). However, we expect fixed-wing UAVs to be more appropriate for connectivity purposes in scenarios where long flight times are necessary (such as for rural coverage), as fixed-wing UAVs rely on a more energy-efficient form of flight when compared to the rotary-wing design. As fixed-wing UAVs are typically incapable of hovering in place, their deployment optimisation involves optimising their individual flight trajectories in a way that allows them to deliver high quality service to the ground users in an energy-efficient manner. In this paper, we propose a multi-agent deep reinforcement learning approach to optimise the energy efficiency of fixed-wing UAV cellular access points while still allowing them to deliver high-quality service to users on the ground. In our decentralized approach, each UAV is equipped with a Dueling Deep Q-Network (DDQN) agent which can adjust the 3D trajectory of the UAV over a series of timesteps. By coordinating with their neighbours, the UAVs adjust their individual flight trajectories in a manner that optimises the total system energy efficiency. We benchmark the performance of our approach against a series of heuristic trajectory planning strategies, and demonstrate that our method can improve the system energy efficiency by as much as 70%.

Index Terms—Cellular-connected UAVs, deep reinforcement learning, energy efficiency.

I. INTRODUCTION

Unmanned Aerial Vehicle (UAV) access points are becoming an attractive option for delivering enhanced wireless coverage in cellular networks [1]. Specifically, UAVs can provide additional capacity to service demand hotspot areas and deliver network coverage in isolated or hard-to-reach rural areas where fixed terrestrial infrastructure may be unavailable or insufficient [1]. UAV infrastructure offers several important advantages to network operators, in that UAVs can be rapidly deployed to provide connectivity to ground users, and leverage their adjustable altitude, obstacle-avoidance capabilities, and strong Line-of-Sight (LoS) communication links to maximise performance.

Despite a growing interest in UAVs, several technical challenges must be addressed to effectively utilise them for each specific networking application. These challenges include

optimising 3D deployment and placement [2], [3], Energy Efficiency (EE) [2], [3], [4], and flight trajectory [5]. Compared to rotary-wing UAVs (such as quadcopters), the fixed-wing UAVs have a better energy-efficient mode of flight due to their mechanical design [6], therefore we anticipate their use for connectivity purposes in scenarios where long flight duration is required, such as for rural coverage. Nevertheless, designing the UAVs to perform their connectivity tasks over extended periods of time is a significant challenge, due to their limited on-board battery energy. At the time of writing, there has been some research into the energy management of fixed-wing UAV systems in relay [7], [8] and data aggregation [4] applications; however, there is a significant lack of research which investigates fixed-wing UAVs acting as flying base stations for delivering coverage.

The work in [7] and [8] propose conventional optimisation methods to maximise the EE of a fixed-wing UAV. However, they only consider a single fixed-wing UAV relay to amplify and forward (AF) received signals between source(s) and destination. In geographically-large rural areas with scattered concentrations of users, multiple fixed-wing UAVs may be deployed [4], [9], [10]. In [4], an iterative method was proposed to optimise the energy consumption of low-power ground devices served by multiple fixed-wing UAVs, by adjusting the UAV trajectories to allow for low-power data transmission from the ground devices. Note that this work focused exclusively on the energy consumption of ground devices, and not the UAVs themselves. Energy consumption of multiple fixed-wing UAVs was optimised in [9], where the authors presented a trajectory planning heuristic to minimise the energy consumption and increase flight time of a network of fixed-wing UAVs that relay data via multi-hop links. The authors demonstrate that increasing the radius of a UAV's circular orbit can reduce the energy consumption for that UAV. The work in [10] proposed deployments that maximise coverage while improving resilience against UAV failure, using circle-packing theory. Note that as [4], [9], [10] focus on basic network coverage scenarios, they do not consider data throughput in their system models, and their optimisation algorithms do not optimise the amount of data that can be delivered across the UAV-user access link.

Reinforcement Learning (RL) has been widely investigated

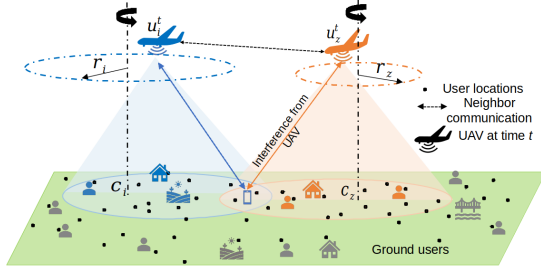


Fig. 1. Fixed-wing UAVs providing wireless coverage to ground devices.

to address the energy management challenge in networks of rotary-wing UAV access points [2], [3]. In [2], a cluster-based Q-learning approach was used to optimise the 3D trajectory of multiple UAVs in the network. A distributed multi-agent Q-learning approach was proposed in our prior work [3] which took into account the interference from neighbouring UAVs. However, the tabular Q-learning technique presented in [2] and [3] may not scale with larger state-spaces, thereby requiring deep RL architectures such as those used in our recent work [11]. It is important to note that rotary-wing UAVs have the advantage of being able to hover in place and move in any direction; this allows for more straightforward trajectory optimisation scenarios. Fixed-wing UAVs, meanwhile, must fly with a certain minimum velocity at all times to remain airborne, and are incapable of making sharp trajectory changes to the same extent as rotary-wing UAVs. For this reason, optimising the system's EE in a network of fixed-wing UAVs is more complex, and requires an entirely different approach.

Motivated by these findings, in this paper we focus on optimising the EE of multiple fixed-wing UAV access points, by balancing both the UAV energy consumption and delivered user throughput. We propose a decentralised, multi-agent RL approach, where each UAV is equipped with a Dueling Deep Q-Network (DDQN) agent which can adjust the UAV flight trajectory. The UAV agent communicates with the agents of its neighbouring UAVs, and uses the obtained information to adjust its trajectory in a way that optimises the overall EE for itself and its neighbours. Unlike prior works, we consider an interference-limited scenario where nearby UAVs can negatively affect user throughput, which allows for a more in-depth optimisation problem. We compare our proposed multi-agent approach against a series of heuristic trajectory planning strategies, under varying sizes of the deployed UAV network. This allows us to demonstrate that our solution is able to optimise the system-wide EE, while still delivering high-quality data throughput to users on the ground. To our knowledge, we are the first to investigate the problem of optimising the EE of fixed-wing UAV access points in an interference-limited multi-UAV network scenario, using tools from deep RL.

II. SYSTEM MODEL

We consider a suburban or rural environment. In this environment there exist a number of users that require cellular service over a certain period of time T . We discretise this time into T timesteps of duration τ . We denote the set of the users

as $\Phi = \{y_1, y_2, y_3, \dots\} \in \mathbb{R}^2$. These users are assumed to be distributed as a homogeneous Poisson point process (PPP). Similar to the related work, we assume the users are static in the environment; the scenario of mobile users is left for a future work.

We assume that a set of UAVs $\mathcal{U} = \{u_1^t, u_2^t, \dots, u_U^t\} \in \mathbb{R}^2$ are deployed by a centralised entity such as a network operator to deliver service to the ground users, with u_i^t denoting the horizontal coordinates of the UAV i at timestep t . This entity has high-level knowledge of the environment, such as the user locations or knowledge about certain points of interest. It uses this information to assign service areas to the UAVs, with the service center-points $\mathcal{C} = \{c_1, c_2, \dots, c_U\} \in \mathbb{R}^2$, where c_i corresponds to the UAV i at location u_i^t . The UAVs are assumed to have a fixed-wing design and cannot hover in place, and so must orbit around their service areas. At timestep t , the UAV i orbits around its center-point c_i with a velocity v_i^t , at a height above ground h_i^t and a radius $r_i^t = \|c_i - u_i^t\|$.

The UAVs have downtilted antennas with cone-shaped coverage patterns. The antenna gain (in dB) from UAV i to user j at timestep t is given as

$$\mu(y_j, u_i^t) = -\min \left(20, 12 \left(\frac{\arctan(\|y_j - u_i^t\|/h_i^t)}{\eta} \right)^2 \right), \quad (1)$$

where η denotes the UAV antenna half-power beamwidth. The users are assumed to have omnidirectional antennas with unitary gain.

In each timestep, each user in Φ associates to the UAV which provides it with the strongest received signal. If at time t the user j is associated with UAV i , the Signal-to-Interference-and-Noise Ratio (SINR) observed by the user is given as

$$\text{SINR}_{i,j}^t = \frac{p c \mu(y_j, u_i^t) ((\|y_j - u_i^t\|)^2 + (h_i^t)^2)^{-\alpha/2}}{\sum_{k \in \mathcal{U} \setminus i} p c \mu(y_j, u_k^t) ((\|y_j - u_k^t\|)^2 + (h_k^t)^2)^{-\alpha/2} + \sigma^2}, \quad (2)$$

where p is the UAV transmit power, c is near-field pathloss, α is the pathloss exponent, and σ^2 is the noise power. Note that, as we are considering UAVs operating in the sky above suburban or rural areas, we assume the wireless channel between the UAVs and the users is always LoS.

Whenever a user j associates with a UAV i we assume it is allocated spectral resources of B bandwidth. As such, the data throughput for user j from UAV i at timestep t is given by the Shannon bound as

$$R_{i,j}^t = \tau B \log_2(1 + \text{SINR}_{i,j}^t). \quad (3)$$

Naturally, $R_{i,j}^t = 0$ for all the UAVs in \mathcal{U} other than i .

At each timestep, the UAV i consumes a certain amount of energy E_i^t given in [6] as

$$E_i^t = \tau \left(\left(c_1 + \frac{c_2}{(g r_i^t)^2} \right) (v_i^t)^3 + \frac{c_2}{v_i^t} \right), \quad (4)$$

where c_1 and c_2 are parameters related to the UAV aerodynamic design [6] and g is the gravitational constant. The UAV

communication equipment will also consume energy, but we assume that this energy consumption is significantly smaller than the energy associated with flight [6], and therefore we only consider the latter in this work. Given the above equation, the velocity which minimises the energy consumption for the given turn radius is derived in [6] as:

$$v^*(r) = \left(\frac{c_2}{3(c_1 + c_2/(gr)^2)} \right)^{1/4}. \quad (5)$$

Note that when the UAV flies at the optimum velocity for its given turn radius, the energy consumption monotonically decreases with increasing turn radius. The EE of UAV i at timestep t is defined as

$$EE_i^t = \frac{\sum_{j \in \Phi} R_{i,j}^t}{E_i^t}. \quad (6)$$

It follows that the total EE of the network across the entire period T is given as

$$EE_{tot} = \frac{\sum_{t=1}^T \sum_{i \in \mathcal{U}} \sum_{j \in \Phi} R_{i,j}^t}{\sum_{t=1}^T \sum_{i \in \mathcal{U}} E_i^t}. \quad (7)$$

III. ENERGY EFFICIENCY OPTIMISATION

A. Problem Statement

When they are deployed by their central entity, the UAVs are assumed to travel to their assigned service areas and enter into a circular orbit around the center-points at the minimum possible turn radius r_{\min} , while delivering service to the users. Once all of the UAVs arrange themselves in this manner (at the beginning of the episode when $t = 1$), each UAV begins to adjust its trajectory around its center-point. In this paper we focus on optimising the UAVs once they arrive at their service areas; optimising UAV trajectories during the initial flight to the center-points is left for a future work. The optimisation problem for the UAV network is given as

$$\max_{(\mathbf{r}_1, \dots, \mathbf{r}_T), (\mathbf{h}_1, \dots, \mathbf{h}_T)} EE_{tot} \quad (8a)$$

$$\text{s.t. } r_{\min} \leq r_i^t \leq r_{\max}, \quad \forall i, t \quad (8b)$$

$$h_{\min} \leq h_i^t \leq h_{\max}, \quad \forall i, t \quad (8c)$$

where $\mathbf{r}_t = (r_1^t, r_2^t, \dots, r_U^t)$ and $\mathbf{h}_t = (h_1^t, h_2^t, \dots, h_U^t)$ are vectors of the UAV radii and heights at timestep t , respectively. In other words, we wish to maximise the total EE of the UAV deployment across the entire episode, by optimising the UAV radii and heights at each timestep. The two constraints ensure that the UAV heights and radii stay within set bounds. As the user locations are assumed to be static the center-points \mathcal{C} are assumed to not change. As such, the UAVs can optimise their EE by adjusting their radii, heights, and velocities. Note that the relationship between the velocity and turn radius is defined as in Eq. (5); we assume that the UAVs are aware

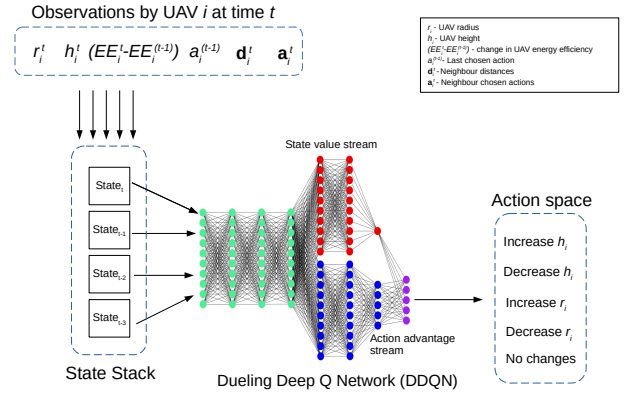


Fig. 2. Our proposed DDQN solution. Note that the number of neurons per DDQN layer is reduced in the diagram for ease of readability.

of this relationship and so always adopt the corresponding velocity for their given turn radius.

B. Solution

To address the optimisation problem defined above, we propose applying a decentralised multi-agent RL solution. Each UAV is equipped with an agent which can gather information about the environment and adjust the UAV trajectory.

For a UAV i , let us denote the set of neighbour UAVs as belonging to the set $\mathcal{U}_i \subset \mathcal{U}$. The set \mathcal{U}_i contains the six UAVs whose center-points are closest to the center-point of i , or all of the UAVs other than i if there are less than six UAVs deployed in total. The reason we consider six UAVs is due to the assumption that when the UAVs are deployed, their service areas will roughly correspond to the shape of a hexagonal lattice, with each UAV being surrounded by a ring of six other UAVs that have the most impact on its throughput via interference.

In each timestep, each UAV agent will communicate with the agents of its neighbouring UAVs and share information. The agents will then use this information to sequentially choose which action to take next. When an agent chooses an action for the current timestep, it broadcasts its choice to its neighbours, so that those neighbours who have not yet chosen an action in the current timestep can use that information for their own decision-making. When all of the agents have decided what action to take next, they will carry out their respective actions simultaneously, transmit their data to the users and consume the corresponding amount of energy each.

We propose using a DDQN for each UAV agent, as depicted in Fig. 2. The DDQN takes in a vector of observations as an input, chooses an action to take, and observes a reward. These are defined below

1) *States*: At timestep t the state \mathbf{s}_t for UAV i is a vector which contains:

- the current UAV turn radius r_i^t .
- its height above ground h_i^t .
- the latest change in the UAV's EE $EE_i^t - EE_i^{(t-1)}$.
- the action taken by i in the previous timestep, $a_i^{(t-1)}$.
- the horizontal distances of the neighbour UAVs in the set \mathcal{U}_i to the center-point c_i at timestep t . We denote

these distances as a vector $\mathbf{d}_i^t = (\|u_1^t - c_i\|, \dots, \|u_j^t - c_i\|), \forall u_j \in \mathcal{U}_i$

- the index of the actions selected by the neighbour UAVs that have already chosen an action to take in this timestep, denoted as the vector $\mathbf{a}_i^t = (a_1^t, \dots, a_j^t), \forall u_j \in \mathcal{U}_i$.

After the state vector \mathbf{s}_t is formed, it is passed into a state stack and combined with the state vectors from the previous three timesteps. This combined vector is then passed into the DDQN. By combining the state vector for multiple timesteps together the agent is able to observe not just the environmental state at that moment, but also the changing dynamics over time based on the chosen actions.

2) *Actions*: Each UAV can take one of five actions at timestep t : increase/decrease the radius by increment r_{inc} , increase/decrease the height by h_{inc} , or keep radius and height the same and continue traveling on its current trajectory. If the UAV changes its radius, it will also adjust its velocity to the one that minimises energy consumption as per Eq. (5).

3) *Rewards*: When all of the agents have chosen which action to take next, all UAV locations are updated for timestep $t + 1$, and the UAVs observe their individual throughput and energy consumption. This performance data is shared among neighbour UAVs, and the reward for the i -th agent at timestep $t + 1$ is calculated as:

$$\rho_i^{(t+1)} = \frac{\sum_{k \in \mathcal{U}_i \cup i} \sum_{j \in \Phi} R_{k,j}^{(t+1)}}{\sum_{k \in \mathcal{U}_i \cup i} E_k^{(t+1)}} - \frac{\sum_{k \in \mathcal{U}_i \cup i} \sum_{j \in \Phi} R_{k,j}^t}{\sum_{k \in \mathcal{U}_i \cup i} E_k^t} \quad (9)$$

In other words, the reward for the i -th agent is the change in the total EE for itself and its neighbours. We assume that by maximising this EE based on local observation data across the different timesteps we will also maximise the total episode EE EE_{tot} .

4) *DDQN implementation*: The DDQN is a neural network which consists of several dense, feedforward neuron layers. There are 4 layers in the main stream, which then split off into a State Value stream and an Action Advantage stream with three layers each, as per the DDQN design [12]. These two streams finally combine together in a combination layer. The combination neuron layer and the final layer of the Action Advantage stream have five neurons each, one for each of the five actions. the final layer in the Value stream has a single neuron. The rest of the layers in the DDQN have 64 neurons. All of the layers with the exception of the combination layer use a ReLU activation function.

5) *DDQN training*: DDQN, like all RL processes, is trained in an online manner. The agent takes actions in the environment, observes the results, and gradually learns how to act to maximise its reward. After an agent takes an action, it stores the previous state stack, the action taken, the received reward, and the new state stack in a database called a replay buffer. After enough timesteps, the replay buffer will be sufficiently populated to use for training. Using uniform random sampling, a batch of entries will be selected from the replay buffer and used to update the weights of the DDQN, following the methodology described in [13, Chapter 4].

TABLE I
NUMERICAL RESULT PARAMETERS

Parameter	Value
Carrier Frequency	2 GHz
pathloss exponent α	2.1
UAV transmit power p	1 W
UAV half-power beamwidth η	30 deg.
UAV mass	10 kg
aerodynamic parameter c_1	$9.26 \cdot 10^{-4}$ [6]
aerodynamic parameter c_2	2250 [6]
Near-field pathloss c	-38.4 dB [14]
Noise power σ^2	$8 \cdot 10^{-13}$ W [14]
User density	10 /km ²
UAV density	0.2 /km ²
UAV height bounds h_{min}, h_{max}	20 m, 300 m
UAV radius bounds r_{min}, r_{max}	50 m, 1000 m
UAV height increment h_{inc}	5 m
UAV radius increment r_{inc}	10 m
MC trials	500
Episodes per MC trial	1
Timesteps per episode T	250
Timestep duration τ	2 seconds
Q-value discount factor	0.1
Learning rate	0.00005
Initial epsilon value ϵ	1
Epsilon decay value	0.99995
Minimum epsilon value	0.001
Replay memory size	5000 entries
Replay batch size	1000

To ensure that the agent is able to explore and populate the replay buffer with a wide range of observations, we use an ϵ -greedy policy, where the agent will take actions randomly with probability ϵ , and will take an action based on the DDQN output otherwise. ϵ has a value of 1 initially, and this is decayed by a certain factor at the end of every timestep. This allows the agent to explore in the beginning of the training process when the DDQN is untrained, while having it rely on the DDQN more and more as it gets better at making decisions.

IV. EVALUATION SCENARIOS AND RESULTS

In this section we evaluate the performance of our proposed algorithm using simulations, across deployments of 2-20 UAVs. We generate a number of Monte Carlo (MC) trials, with a random distribution of users in each trial distributed in a square simulation area of a certain size. To preserve the UAV and user densities, we scale up the size of the simulation area with the increasing number of deployed UAVs, with simulation areas in the range of 10-100 km², and user numbers in the order of 100-1000. The center-points are found for a given user distribution and number of deployed UAVs using the K-Means Clustering algorithm [15]. The UAVs are deployed in a circular orbit around their center-points, at an initial height of 100 m and the minimum possible radius r_{min} . The reason we initialise the UAVs to fly at the minimum radius is that this ensures they are as close as possible to the center-points, and therefore can achieve the highest throughput to the users, but at the worst possible energy consumption. The training episode will then begin, and the UAVs act to optimise their flight trajectories with respect to the system EE. The numerical result parameter values are given in the table. Fig. 3 shows an example of the UAV orbits for one of the MC trials.

As the problem of optimising the EE of fixed-wing UAV access points in an interference-limited environment is quite

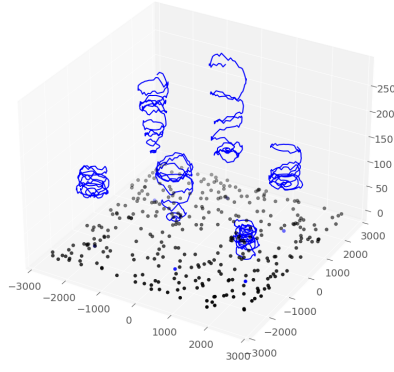


Fig. 3. 3D orbits of six deployed UAVs following our proposed algorithm. novel, there is a lack of available benchmarks against which to compare the performance of our multi-agent solution. As such, we propose several heuristics for the results comparison:

- Minimum radius orbit. For this heuristic the UAVs remain at their initial heights and turn radii, and follow their simple circular orbits for the entire episode.
- Quadcopter-style UAV hovering above the center-points. For this heuristic, the UAVs are assumed to have a quadcopter design, and are assumed to hover in place directly over their center-points throughout the episode, as in [15]. This represents the type of UAV access point network most commonly investigated in the literature, due to their flexible mobility and hovering capability. To model their energy consumption, we use Eq. (2) in [16].
- Bounded random walk. In this heuristic, the UAVs choose their actions randomly in each timestep, provided the heights and radii remain within the permitted bounds. As our RL solution relies on ϵ -greedy exploration during training, this benchmark represents the performance bound of our solution before it is trained.
- Energy-saving orbit. In this heuristic, all of the UAVs fly in simple orbits at a radius equal to half the minimum distance between two center-points. This represents the maximum orbits that the UAVs can fly at without any overlaps occurring, and is aimed at minimising the energy consumption.

Fig. 4 shows how our algorithm performs as it is trained over a number of episodes. To improve the clarity of our results, for each episode the overall system performance results of the algorithm and the heuristics are normalised with respect to the performance of the minimum radius orbit heuristic. This allows us to display the results as ratios of the minimum radius baseline. We observe that in the beginning of the training process, our algorithm (shown in red) relies on random action exploration according to the ϵ -greedy policy, and as such gives performance comparable to the bounded random walk heuristic (shown in blue). However, after approximately 100 episodes the algorithm reaches a point where it can reliably outperform all of the heuristics that we test against. Note that each episode corresponds to its own MC trial, which means that for each episode we randomise the positions of the ground users, and recalculate the center-points for the UAVs. As a result, the performance fluctuates from episode to episode. It

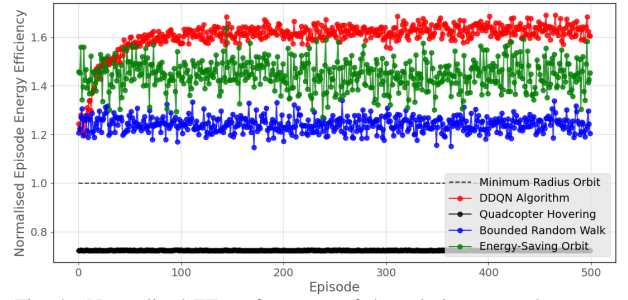


Fig. 4. Normalised EE performance of the solutions over the range of episodes, given 10 UAVs.

is important to note that our algorithm is able to deal with this randomness, and is able to give good performance even when applied to a "new" environment with user distributions that it had not been trained on previously.

To verify that our algorithm can scale for varying numbers of deployed UAVs, we generate our numerical results for a range of UAV fleet sizes. For each fleet size, we rerun our training process for 500 episodes, and record the normalised performance metrics for the 400 episodes after training concludes. The resulting mean values for EE, episode throughput, and energy consumption are shown in Fig. 5 to Fig. 7.

Our first observation is that the fixed-wing UAV deployments, and our proposed algorithm in particular, all significantly outperform the hovering quadcopter heuristic in terms of EE across the entire range of UAV deployments. This is explained by investigating the throughput and energy consumption figures. Fig. 6 shows that hovering directly over the center-points instead of maintaining a close orbit around them gives minimal improvement to the resulting user channel throughput. However, Fig. 7 shows that hovering directly in place consumes substantially more energy than the fixed-wing UAVs, as the hovering UAVs cannot benefit from the effect of aerodynamic lift, and must instead generate enough downward thrust to counter the force of gravity. This is in line with real-world UAV performance, and once more highlights the importance of using fixed-wing designs in scenarios where the UAVs must stay in the air for extended periods of time.

The figures also show that our algorithm consistently gives the best EE performance, compared to the other heuristics. The algorithm is able to deliver up to 70% more EE compared to the minimum radius orbit baseline. We also note that increasing the number of UAVs in the network reduces the gains by only approximately 10%. As expected, the majority of the interference for a UAV comes from its six closest neighbours, and as such the UAVs can successfully optimise the global performance based only on the local observations from their nearest neighbours.

Looking at Fig. 6 we see that optimising the EE does result in the DDQN algorithm sacrificing some throughput, but this appears to be only in the order of a couple of percent compared to the hovering or minimum radius orbit performance. Overall, the UAV network is able to maintain consistently high-quality throughput for the ground users.

The real performance gains arise from the energy consump-

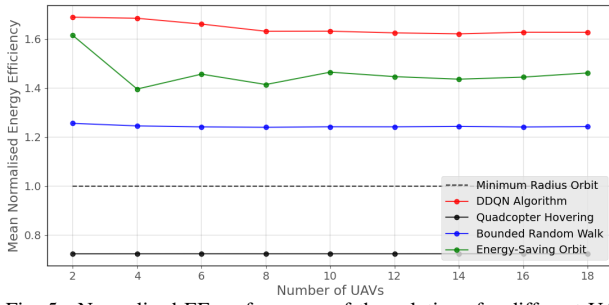


Fig. 5. Normalised EE performance of the solutions for different UAV numbers.

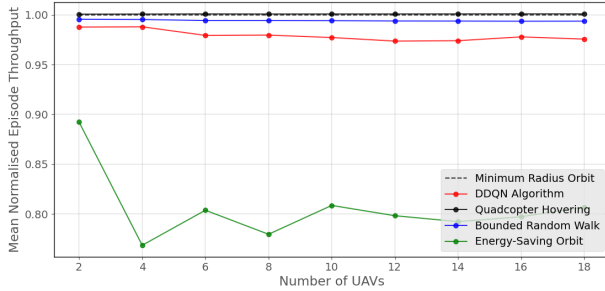


Fig. 6. Normalised system throughput performance of the solutions for different UAV numbers.

tion, shown in Fig. 7. By intelligently adjusting their flight trajectories, the UAVs with the DDQN algorithm are able to intelligently increase their orbit radii and reduce their energy consumption by approximately 40% compared to the baseline. Note that the bounded random walk heuristic also manages to reduce the energy consumption by randomly drifting away from the center-points.

Finally, we observe that the energy-saving orbit heuristic is able to give good performance, but only for very small numbers of UAVs when the aggregate interference is low. As the UAVs fly far away from their center-points they are significantly more vulnerable to interference than the other deployment strategies which fly closer to the center-points. Note that there is some fluctuation in the performance for 4-10 drone scenarios, we attribute this to the variable orbit distances that arise from placing wide, non-overlapping UAV orbits in square simulation areas.

V. CONCLUSION

In this work we have demonstrated a multi-agent deep RL approach to optimise the EE of a fleet of fixed-wing UAV access points that are deployed to provide service to ground users, under interference-limited channels. We demonstrated that our proposed solution can significantly improve the system EE based on local state observations and communication between neighbouring UAVs, while still ensuring that ground users receive high-quality service. In future works, we will extend our study to consider scenarios where users move through the environment, such as high-speed road users. For these scenarios, we will investigate how to optimise the flights of the UAVs to accommodate multiple types of users. In this work we have focused on the ground user access link; in future works, we may also optimise around the wireless backhaul of the UAVs.

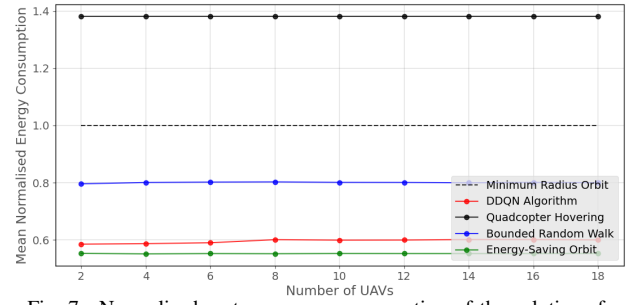


Fig. 7. Normalised system energy consumption of the solutions for different UAV numbers.

REFERENCES

- [1] M. Mozaffari, W. Saad, M. Bennis, Y. Nam, and M. Debbah, "A Tutorial on UAVs for Wireless Networks: Applications, Challenges, and Open Problems," *IEEE Communications Surveys & Tutorials*, vol. 21, no. 3, pp. 2334–2360, Third Quarter 2019.
- [2] X. Liu, Y. Liu, and Y. Chen, "Reinforcement Learning in Multiple-UAV Networks: Deployment and Movement Design," *IEEE Transactions on Vehicular Technology*, vol. 68, no. 8, pp. 8036–8049, Aug. 2019.
- [3] B. Omoniwa, B. Galkin, and I. Dusparic, "Energy-Aware Placement Optimization of UAV Base Stations via Decentralized Multi-Agent Q-Learning," *IEEE Consumer Communications & Networking Conference (CCNC) (to appear)*, Jan 2022.
- [4] Y.-C. Kuo, J.-H. Chiu, J.-P. Sheu, and Y.-W. P. Hong, "UAV Deployment and IoT Device Association for Energy-Efficient Data-Gathering in Fixed-Wing Multi-UAV Networks," *IEEE Transactions on Green Communications and Networking*, pp. 1–1, June 2021.
- [5] A. Visintini, T. D. Perera, and D. N. K. Jayakody, "3-D Trajectory Optimization for Fixed-Wing UAV-Enabled Wireless Network," *IEEE Access*, vol. 9, pp. 35 045–35 056, Feb. 2021.
- [6] Y. Zeng and R. Zhang, "Energy-Efficient UAV Communication with Trajectory Optimization," *IEEE Transactions on Wireless Communications*, vol. 16, no. 6, pp. 3747 – 3760, March 2017.
- [7] K. Song, J. Zhang, Z. Ji, J. Jiang, and C. Li, "Energy-Efficiency for IoT System with Cache-Enabled Fixed-Wing UAV Relay," *IEEE Access*, vol. 8, pp. 117 503–117 512, June 2020.
- [8] S. Ahmed, M. Z. Chowdhury, and Y. M. Jang, "Energy-Efficient UAV Relaying Communications to Serve Ground Nodes," *IEEE Communications Letters*, vol. 24, no. 4, pp. 849–852, Jan. 2020.
- [9] Y. W. Peter Hong, R. H. Cheng, Y. C. Hsiao, and J. P. Sheu, "Power-Efficient Trajectory Adjustment and Temporal Routing for Multi-UAV Networks," *IEEE Transactions on Green Communications and Networking*, vol. 4, no. 4, pp. 1106–1119, Aug. 2020.
- [10] S. Shrivastav and Z. Song, "Coordinated Coverage and Fault Tolerance using Fixed-wing Unmanned Aerial Vehicles," *2020 International Conference on Unmanned Aircraft Systems, ICUAS 2020*, pp. 1231–1240, Sept. 2020.
- [11] B. Galkin, E. Fonseca, R. Amer, L. A. DaSilva, and I. Dusparic, "RE-QIBA: Regression and Deep Q-Learning for Intelligent UAV Cellular User to Base Station Association," *IEEE Transactions on Vehicular Technology (to appear)*, p. arXiv:2010.01126, Oct. 2020.
- [12] Z. Wang, T. Schaul, M. Hessel, H. Hasselt, M. Lanctot, and N. Freitas, "Dueling Network Architectures for Deep Reinforcement Learning," *International Conference on Machine Learning*, June 2016.
- [13] V. François-Lavet, P. Henderson, R. Islam, M. G. Bellemare, and J. Pineau, "An Introduction to Deep Reinforcement Learning," *Foundations and Trends in Machine Learning*, vol. 11, no. 3-4, 2018.
- [14] H. Elshaer, M. N. Kulkarni, F. Boccardi, J. G. Andrews, and M. Dohler, "Downlink and Uplink Cell Association With Traditional Macrocells and Millimeter Wave Small Cells," *IEEE Transactions on Wireless Communications*, vol. 15, no. 9, pp. 6244–6258, Sept. 2016.
- [15] B. Galkin, J. Kibilda, and L. A. DaSilva, "Deployment of UAV-Mounted Access Points According to Spatial User Locations in Two-Tier Cellular Networks," *2016 Wireless Days (WD)*, March 2016.
- [16] N. Kingry *et al.*, "Design, Modeling and Control of a Solar-Powered Quadcopter," *IEEE International Conference on Robotics and Automation (ICRA)*, pp. 1251–1258, May 2018.